Exosomes Derived from Anoxia Preconditioned Mesenchymal Stem Cells alleviate Myocardial Ischemia Reperfusion Injury by Inhibiting Pyroptosis/ Caspase-1 Induced Apoptosis in The Deficiency of Gasdermin D

Chengyu Mao
Shanghai Jiao Tong University School of Medicine
Dongjiu Li
Shanghai Jiao Tong University School of Medicine
En Zhou
Shanghai Jiao Tong University School of Medicine
Erhe Gao
Lewis Katz School of Medicine at Temple University
Tiantian Zhang
Shanghai Jiao Tong University School of Medicine
Lin Gao
Shanghai Jiao Tong University School of Medicine
Kan Chen
Shanghai Jiao Tong University School of Medicine
Yue Wang
Shanghai Jiao Tong University School of Medicine
Changqian Wang (wangcqdr1218@163.com)
Shanghai Jiao Tong University School of Medicine

Research

Keywords: Myocardial ischemia reperfusion injury, mesenchymal stem cells, exosomes□pyroptosis-induced apoptosis, GSDMD deficiency

Posted Date: August 18th, 2020

DOI: https://doi.org/10.21203/rs.3.rs-57443/v1

Abstract

Background

Exosomes derived from adipose-derived mesenchymal stem cells can potentially protect cardiomyocytes from myocardial ischemia reperfusion injury. It's notable that exosomes derived from adipose-derived mesenchymal stem cells underwent anoxia preconditioning showed a better cardioprotective effect than that without anoxia. Here, in vitro and in vivo studies were used to investigate the cardioprotective effects against myocardial ischemia reperfusion injury of exosomes derived from adipose-derived mesenchymal stem cells with (Int-EXO) or without anoxia (NC-EXO), respectively.

Methods: Adipose-derived mesenchymal stem cells and exosomes were identified by western blot, flow cytometry, transmission electron microscopy, and nanosight. An exosome tracer assay identified exosomes absorbed by cells. An *in vitro* model using mice cardiomyocytes for studying anoxia-reoxygenation and an *in vivo* mice model of MIRI were used to investigate the cardioprotective effects of NC-Exo and Int-Exo, respectively.

Results

We discovered that treatment with NC-EXO and Int-EXO significantly reduced the infarct size and attenuated cardiomyocyte apoptosis, In addition, Int-EXO group had a less infarct size and apoptosis degree. The mechanism revealed by RNA sequencing showed that 40 miRNAs were up-regulated in Int-EXO compared to NC-EXO. 10 of these miRNAs could bind thioredoxin-interacting protein as a downstream target gene; among these, the top-discrepant miRNA224-5p was selected for further study. Dual luciferase reporter assay and rescue study verified TXNIP as a target gene for miR-224-5p. Furthermore, the cellular death signaling pathway which Int-EXO involved in mediating was in a special form of apoptosis, not pyroptosis, induced by activated thioredoxin-interacting protein-pyroptosis-caspase1 pathway in gasdermin D-deficient cells.

Conclusion

The research demonstrated adipose-derived mesenchymal stem cells exosomes attenuated MIRI by inhibiting pyroptosis-induced apoptosis in cardiomyocytes which are lack of gasdermin D. The cardioprotective effect of Int-EXO was more significant than that of NC-EXO, possibly due to treated with anoxia preconditioning, adipose-derived mesenchymal stem cells product more miRNAs targeting thioredoxin-interacting protein in exosomes to alleviate pyroptosis-induced apoptosis. These findings provide new insights into the pathogenesis and methods for intervention of myocardial ischemia reperfusion injury.

Highlights

- Exosomes from ADSCs which underwent intermittent anoxia preconditioning exerted significant cardioprotective effects against MIRI.
- ADSCs upregulate miRNAs tageting to TXNIP in exosomes,which may contribute to cardioprotection effects of Int-Exo.
- Activating TXNIP would induce apotosis in cardiomyocytes rather than pyroptosis, because of the deficiency of GSDMD in cardiomyocytes.
- Our study partly explained the link between pyroptosis and apoptosis, Which may promote clinical transformation of this particular exosomes.

1. Introduction

Myocardial ischemia reperfusion injury(MIRI) is caused by blood flow reperfusion after continuous myocardial ischemia due to excessive oxygen free radical formation, calcium overload, and other mechanisms that influence the curative effect of reperfusion therapy[1]. Although great advancements in pharmacological and interventional therapies have been made to revascularize infarct-related arteries, MIRI, which is caused by secondary oxidative-stress damage in the myocardium, remains a major challenge in the clinical practice[2, 3]. There is an unmet need to alleviate MIRI after infarct-related artery revascularization.

Emerging evidence points to a potential molecular mechanism for MIRI[4, 5]. Secondary oxidative-stress damage in the myocardium triggered by excessive production of mitochondrial reactive oxygen species (mROS) is accompanied by revascularization of the infarct-related artery[4, 6]. Moreover, sustained and excessive mROS production is a particular mediator of pyroptosis, which stimulates inflammasomes to join together and cleave caspase-1; this, in turn, triggers an inflammatory response that leads to the progression of MIRI[7]. Not only that, cleaved caspase-1 inhibits the activity of transcription factor GATA4[8], which is closely related to heart development and is a link between pyroptosis and apoptosis to initiate comprehensive programmed cell death in the myocardium. Therapeutics targeting pyroptosis protect the ischemic-reperfusion injured heart from sterile inflammation, apoptosis, and dysfunction[9, 10]. In addition, mROS has also been demonstrated to upregulate thioredoxin-interacting protein (TXNIP), which in turn represses the activity of hypoxia inducible factor-1, hence weakening myocardial tolerance to anoxia and inducing the formation of inflammasomes[11]. These findings highlight the contributions of mROS in the induction of myocardial pyroptosis and apoptosis; however, the underlying mediators require further elucidation.

Exosomes, which are lipid bilayer extracellular vesicles with diameters ranging from 30 nm to 150 nm, are released by almost all types of cells including mesenchymal stem cells. They can modulate intercellular communications by transferring proteins, mRNAs, and miRNAs between cells, and they have the potential for cell-specific targeting[12]. Exosomes derived from cells in different stages, states, species, and environments have distinct inclusions[13]. The process of exosomal action usually inherits the biological characteristics of the source cell to intervene in the trajectories of various physiological and pathological

processes, including cell proliferation, differentiation, secretion, migration, and death. Changes in microenvironment and the state of cells can enhance or weaken the biological function of secreted exosomes. Exosomes have been reported to be important regulators of various cardiovascular diseases[14]. For example, exosomes derived from mesenchymal stem cells have the potential of protecting cardiomyocytes from MIRI and non-specific inflammation[15]. Cardiac fibroblast-derived exosomes facilitate pathological cardiac hypertrophy via activating the renin angiotensin system in cardiomyocytes[16], and exosomes derived from cardiomyocytes contribute to cardiac fibrogenesis via myocyte-fibroblast cross-talk[17]. Obviously, the cell source of exosomes greatly determines their action modality and functional outcome.

Given the fact that anoxia preconditioning can enhance cardiomyocyte tolerance against an oxygen-deficient environment, inflammation, and oxidative stress[18, 19], we hypothesized that exosomes derived from mesenchymal stem cells undergoing ischemic preconditioning have a more significant potential to ameliorate MIRI, oxidative stress damage, and sterile inflammation. We demonstrate that exosomes derived from adipose-derived mesenchymal stem cells (ADSCs) pretreated with anoxia preconditioning could be absorbed by cardiomyocytes and thereby ameliorate pyroptosis/caspase-1 induced apoptosis. Interestingly, these exosomes show a more significant cardioprotective effect than ADSCs without anoxia preconditioning. Furthermore, we showed that miR-224-5p is enriched in ADSCs-derived exosomes pretreated with anoxia preconditioning and that TXNIP is a downstream target of miR-224-5p, which can bind to and inhibit the antioxidant protein thioredoxin and is a key event linked to NLRP3 inflammasome via reactive oxygen species[20, 21]. Inhibition of TXNIP can suppress the activation of inflammasomes and pro-caspase-1, thus ameliorating pyroptosis, perpetuating GATA4 levels in cardiomyocytes, and alleviating cardiomyocyte apoptosis, which just existed in GSDMD-deficient cells.

2. Materials And Methods

2.1. Animal studys and mice model of MIRI

All animal experiment procedures after appraisals, feasibility studies were approved by the Shanghai Ninth People's Hospital institutional ethics committee (SH9H-2017-A39-1). All experimental contents acted in accordance with the guidelines of the Directive 2010/63/EU of European Parliament. Six weeks old male specific pathogen free(SPF) Wild-type (WT) C57BL/6 mice were purchased from Experimental Animal Center of Shanghai Ninth People's Hospital. The mice were fed normally under SPF conditions in experimental animal center until eight weeks. Mice were firstly induced anesthesia in an anesthesia box with 3% concentration of isoflurane(Sinopharm Chemical reagent co.,Ltd, Shanghai, China) for 1 minites and then mice were maintained anesthesia with 1.5-2% concentration of isoflurane through an anaesthetic mask. After mice were under complete anesthesia, invasive experiments were allowed to carry out. In order to minimize potential errors, animal operations(model of MIRI, Evensblue/TTC stain) were performed by Professor Erhe gao(MD,PhD,Director of Small Animal Surgery and Physiology Core, Lewis Katz School of Medicine, Temple University, USA). Mice were euthanized with excessive carbon dioxide inhalation.

A total of 80 healthy (WT C57BL/6) male mice (eight weeks old, ~ 24 g) were kept under SPF experimental animal feeding surroundings (temperature, 20-24^{o}C; humidity, 50–60), and fed with standard mouse chow and water ad with ad libitum feeding. Mice model of MIRI was operated under anesthesia with 1.5-2% concentration of isoflurane through an anaesthetic mask by ligating the left coronary artery (LCA) for 30 min with a silpknot, then released the slipknot to induce reperfusion. Successful model of MIRI was confirmed by electrocardiograph(ECG) dynamic changes (ST segment elevation). After releasing the slipknot ligating LCA with a certain period of time, that is blood reperfution, hearts were harvested for further studys. A sham operated group was used as a control and underwent the same procedure, with the exception that the knot was left untied. For a detailed description of the procedure, please review Gao et al., 2010 [22].

2.2. Transthoracic echocardiography

Echocardiography was applied to assess on the baseline(day0), 1st, 3rd and the 7th day after reperfusion by using a Vevo 770 high-resolution imaging system. After mice were anaesthetized with 1.5-2% concentration of isoflurane, echocardiography assessment was carried out to evaluate cardiac function. The ejection fraction (EF) and fractional shortening (FS) on the baseline(day0), 1st, 3rd and the 7th day were measured.

2.3. Evaluation of area at risk and infarct size

After reperfusion for 4 hours, the chest wall was reopened to expose the heart after mice were anaesthetized with 1.5-2% concentration of isoflurane through mask. The LCA was re-ligated at the same degree of previous ligation, and 1% Evans Blue was injected through the ascending aorta with the distal artery nipped until the non-infarction zone turned blue. The heart was harvested, washed in saline, and sliced horizontally into five pieces from left ventricular apex to the degree of ligation. All tissue pieces were incubated in 1% TTC for 20 min at 37 °C. Image Pro Plus 6.0 was used to calculate infarct area and area at risk(AAR). AAR/ left ventricle area (LV) and infarct size (IS) /AAR were analized.

2.4. Isolation and culture of mouse adipose-derived stem cells

Mesenchymal stem cells were harvested from C57BL/6 mice adipose tissue, as previously described[23]. In brief, adipose tissue isolated form proximal limb was digested by 0.075% collagenase IV(9001-12-1; Sigma, USA) for 60 min at 37 °C in a mechanical horizontal rotator at a speed of 180 rpm/min. The collagenase IV was dissolve in complete medium contained DMEM/F12(SH30023.01; Hyclone, USA) and 10% fetal bovine serum (FBS, ST303302, PAN, Germany). Then the mixture was centrifugated at a speed of 200 × g for 10 min. After centrifugation the supernatant was discarded and the cell pellet was resuspended in complete medium(DMEM/F12 and 10% exosome-free serum). The medium was placed in incubator at 37 °C in a 5% CO_2 atmosphere[23] for three days without taking out or shaking.

2.5. Isolation and culture of neonatal mice cardiomyocytes

Cardiomyocytes were isolated from 1 to 2 day-old C57BL/6 mice as described previously[24]. In Brief, mice were disinfected quickly in a 75% ethanol solution, and hearts were quickly extracted and digested in 0.125% concentration trypsin diluted with PBS (15090-046,Gibco.USA) at 4 °C overnight. Subsequently, supernatant was collected and centrifuged at 200 × *g* for 5 min and the cell pellet was cultured in DMEM containing 10% FBS at 37 °C in a 5% CO2 atmosphere. After 1.5 hour of incubation to induce fibroblast adhering on dishes, then supernatant containing cardiomyocytes were plated in 0.1% gelatin-coated dishes in a density of 1×10^6 cells/mL. The purity of isolated cardiomyocytes was estimated by α-actinin staining (Fig. 1B).

2.6. Anoxia/ reoxygenation model of cardiomyocytes

To establish Anoxia/ reoxygenation model of cardiomyocytes, cardiomyocytes were incubated in oxygen-free DMEM medium(low glucoce) in an atmosphere content of 95%N2 and 5%CO2 for 2 h,then recovering oxygen and replacing oxygen–normal DMEM(low glucoce) medium for 1 h.

2.7. ADSCs treated with anoxia preconditioning

ADSCs were seeded at $1–2 \times 10^6$ cells/100-mm cell-culture dishes in exosome-free complete medium for 24 h, then medium was exchanged for DMEM/F12 which was incubated with 100%N2 overnight to remove oxygen existed in medium as possible. For anoxia preconditioning, the cells were subjected to repeated cycles of anoxia (60 min with oxygen-free medium) with intermittent reoxygenation (30 min with normal DMEM/F12) for five cycles in an anoxic chamber(Forma-1025 Anaerobic System, Thermo, USA). Then ADSCs were incubated with serum-free medium in normal cultivation environment(21%O2, 5%CO2) and supernate was collected after 24 h.

2.8. Isolation and characterization of exosomes

Exosomes were isolated by differential centrifugation in conditioned media. In brief, the cell supernatant was centrifuged at 2,000 × *g* for 30 min at 4 °C to remove cell debris and cell fragments; cell supernatant was then collected and centrifuged at 100,000 × *g* for 70 min to precipitate exosomes to the bottom of centrifuge tube. After that, supernatant was discarded in order to remove the contaminated protein, and exosomes were suspended in PBS and centrifuged at 100,000 × *g* for 70 min. Finally, the sub-packaged precipitates were preserved at − 80 °C; repeated freeze/thaw cycles were avoided. Size distribution and concentration of exosomes were verified by a NanoSight NS300 instrument (Malvern Instruments, Malvern, UK), and the morphology of exosomes was defined using transmission electron microscopy (TEM) (Fig. 1G). Expression of the exosomal markers TSG101, CD9 (positive controls), and calnexin (negative control) was assessed by western blot[25].

2.9. Exosomes Injection

Mice were randomly divided into 4 groups including sham group (n = 20), MIRI group (n = 20), NC-Exo group (n = 20), and Int-Exo group (n = 20). The groups were handled under the following conditions: 1) sham group mice undergoing sham surgery; 2) MIRI group mice undergoing coronary artery ligation for

30 min, followed by reperfusion for an appropriate time; 3) NC-Exo group mice undergoing coronary artery ligation for 30 min and drawing out the suture to loose the slipknot for reperfusion, then NC-Exo (10 μg per gram of body weight) were injected through the tail vein; 4) Int-Exo group mice undergoing coronary artery ligation for 30 min and drawing out the suture to loose the slipknot for reperfusion, then Int-Exo (10 μg per gram of body weight) were injected through the tail vein.

2.10. Analysis of exosomes uptake into cardiomyocytes

Exosomes and mice cardiomyocytes were labeled with PKH67 (MINI67, Sigma-Aldrich,USA) and phalloidin (A12379s, ThermoFisher,USA), respectively, according to the manufacturer's protocol. A total of 5 μL of PKH26-stained exosomes was added to the sample, followed by a 2 hours incubation for internalization by the cell. After washing twice with PBS, slides were fixed in 4% paraformaldehyde and cell nuclears were stained with DAPI (C1005, Beyotime, China). Fluorescent images were collected by using a inverted microscope (BX63, Olympus, Japan) at x□630 magnification (Fig. 1F).

2.11 Cell transfection

Cells were seeded in a 6- or 24-well plate, and transfected with miR-224-5p mimics, inhibitors, or plasmid DNA using a Lipofectamine 3000 transfection reagent (Cat. 11668019,Invitrogen,USA) following the manufacturer's protocol. Experiments were performed 24 h after transfection.

2.12 Immunofluorescence assay

Cells cultured on confocal plates were fixed in 4% paraformaldehyde for 15 min, then washed with PBS for 3 times, and cells were permeabilized with 0.5% Triton X-100(C1016, Beyotime, China) for 15 min. Cells were blocked with a primary antibody dilution buffer for 1 hour at room temperature. Next, cells were incubated with mice anti-α-actinin primary antibody (1:1000, ab9465, Abcam,USA) overnight at 4 °C. Primary antibody was removed and the cells were washed twice with PBS. Then, the cells were incubated with a secondary antibody (1:1000, 4409, CST,USA) for 2 hours at room temperature. The cells nuclears were then stained with DAPI for 5 min at room temperature. Fluorescent images were collected by using a inverted microscope (BX63, Olympus, Japan) at x□630 magnification.

2.13 Dual luciferase reporter assay

HEK 293T cells were cultured in a 24-well plate. When cell confluence reached approximately 70%, cells were transfected with PGL3 luciferase plasmids containing WT, NC and mutated TXNIP 3'UTR and miR 224-5p mimic (Ribobio, Shanghai, China). Then cells were re-cultured in a lucifugal 96well plates 12 hours later. After 36 hours, the ratio of fireflyluciferase and ranilla luciferase was detected using the Dual-GLO™ Luciferase Assay System (E2920,Promega,USA).

2.14 Real-time PCR

Total RNAs were extracted with RNAiso Plus extraction reagent following the manufacturer's instructions (No. 9108, Takara, Dalian, China). Stem-loop primers(purchased from Ribobio Biotech, guangzhou, China)

were used to produce cDNA of miRNA by using PrimeScriptTM RT reagent Kit (RR047A, Takara, Dalian, China). The miRNA-cDNA was amplified by using TB Green® Premix Ex Taq™ II (RR820L, Takara, Dalian, China) through ABI-7500 Real-Time PCR Detection System (Applied Biosystems, USA). U6 was used as an internal control.

2.15 Western blotting

Protein was extracted from cardic tissues, cardiomyocytes. 10ug total protain was separated on 12% SDS-PAGE at 80 V for 1.5 hour, and then transferred to a PVDF membrane (IPVH00010,Millipore,USA) at 300 mA for 1 hour. After blocking. Membranes were incubated with primary antibodies at 4 °C overnight and secondary antibodies at room temperature for 1 hour. The primary antibodies used in the study included rabbit anti-TSG101 (1:2000, ab125011, Abcam,USA), rabbit anti-CD9 (1:2000, ab92726, Abcam,USA), rabbit anti-TXNIP (1:1000, ab188865, Abcam,USA), rabbit anti-ASC (1:1000, 67824, CST,USA), rabbit anti-caspase-1 (1:1000, ab179515, Abcam,USA), rabbit anti-GATA4 (1:1000,ab134057,Abcam,USA), rabbit anti-BCL-2 (1:1000, #3498, CST, USA), rabbit anti-BAX (1:1000, #2772, CST, USA), rabbit anti-caspase-3(1:1000, #14220, CST, USA), rabbit anti-α-actinin (1:1000, ab9465, Abcam, USA), and rabbit anti-α-tubulin (1:1000, #2125, CST, USA). Immunoreactive proteins were visualized using ECL substrate kit (ab65623, Abcam, USA) and two-color infrared fluorescence imaging system(Odyssey CLX, LICOR, USA). Tubulin-α was applied as internal control.

2.16 Statistical analysis

Data analysis was performed through SPSS 19.0 software. Shapiro-Wilk test was applied to assess whether data conformed to normal distribution. Statistical analysis was performed using Pearson Chi square test($n \geq 5$) or Fisher exact test($n \leq 5$)with subsequent multiple comparisons using Chi square with Bonferroni correction for categorical variables. One-way ANOVA with subsequent post hoc multiple comparisons using the Student-Newman-Keuls test for continuous variables. Kruskal–Wallis test was applied to nonparametric testing of multiple independent samples and a Dunn-Bonferroni test for post hoc comparisons.

3. Results

3.1. Identification of ADSCs and ADSCs-derived exosomes.

To examine whether ADSCs were successfully isolated from mice adipose tissue, we used CD29, CD45, and CD90 as cell surface markers, and CD34, CD105, and CD106 as negative controls. As shown in Fig. 1A, more than 95% of cells isolated from adipose tissue were positive for surface markers (CD29, CD45, and CD90) and hardly express the negative markers (CD34, CD105, and CD106). Subsequently, exosomes were obtained through sequential centrifugation and characterized by nanosight and transmission electron microscope and TEM to confirm the diameters of vesicles (ranging from 50 to 150 nm, with a median average size 115 nm) (Fig. 1C,E). The isolated vesicles also contained the

exosome-associated markers (CD9, CD63, and tumor susceptibility gene (TSG101)), but did not contain calnexin (Fig. 1D).

3.2. Exosomes derived from ADSCs with anoxia preconditioning alleviated pyroptosis in cardiomyocytes

To confirm whether ADSCs-derived exosomes with anoxia preconditioning (Int-Exo) can more markedly influence pyroptosis in MIRI,pyroptosis pathway was detected in cardiomyocytes. As shown in Fig. 2(A-B), Int-Exo and exosomes derived from untreated ADSCs (NC-Exo) decreased the expression of TXNIP, and cleaved- caspase-1 (TXNIP, cleaved-caspase1; NC-Exo vs IR group, $p = 0.0007$, $p = 0.0002$, respectively; Int-Exo vs NC-Exo group, $p = 0.0194$, $p = 0.0007$, respectively)

3.3. Exosomes derived from ADSCs with anoxia preconditioning ameliorated apoptosis in cardiomyocytes

It has been proven that cleaved caspase-1 can deactivate GATA4 which is a key transcription factor closely related to heart development and inhibition of apoptosis[8]. To explore the biological functions of the pyroptosis-GATA4-apoptosis axis, we conducted an Annexin V-PI assay and Western blot to evaluate the influence of Int-Exo and NC-Exo on cardiomyocyte apoptosis. As shown in Fig. 2(C-F), Int-Exo and NC-Exo decreased the protein expression of cleaved-caspase-3 and upregulated the protein expression of GATA4, Bcl-2/Bax in cardiomyocytes (NC-Exo vs IR group; GATA4, Bcl-2/Bax, cleaved-caspase-3, $p = 0.036$, $p = 0.0007$, $p = 0.0058$, respectively; Int-Exo vs NC-Exo group; GATA4, Bcl-2/Bax, cleaved-caspase-3, $p = 0.0106$, $p = 0.0022$, $p = 0.0003$,respectively) treated with anoxia-reoxygenation. Meanwhile, the Annexin V-PI assay demonstrated a downward tendency of apoptotic cell ratio in Int-Exo and NC-Exo groups with anoxia and re-oxygenation. Meanwhile, he the Int-Exo group showed a lower percentage of apoptotic cells (NC-Exo vs IR group; $p = 0.0002$; Int-Exo vs NC-Exo group; $p = 0.0143$).

3.4. Cardiomyocytes exhibit a lower expression level of GSDMD

To verify the final result of activation of TXNIP-pyroptosis/caspase-1 pathway being in the form of apoptosis rather than GSDMD-induced-pyroptosis in cardiomyocytes, which may partly caused by the deficiency of GSDMD, we investigated the expression differences of GSDMD in cardiomyocytes and myeloid cells(Fig. 2G-H). Results of western blot exhibit that pretreated with anoxic/reoxygenation, no differences of cleaved GSDMD expression between CM and CM + IR group($p = 0.991$). Meanwhile,stimulated with anoxic/reoxygenation, expression of GSDMD in RAW264.7 + IR group was significant higher than that in CM($p < 0.0001$), CM + IR group($p < 0.0001$) and RAW264.7 group($p < 0.0001$). In addition, no differences of total GSDMD expression were detected between CM and CM + IR group($p = 0.9898$). However, total GSDMD expression in RAW264.7 group is much more higher than that in CM group($p < 0.0001$) and same trend was observed in CM + IR and RAW264.7 + IR group($p < 0.0001$).

3.5. ADSCs-derived exosomes with anoxia preconditioning ameliorated in-situ apoptosis in MIRI

To further validate the anti-apoptotic effects of NC-Exo and Int-Exo *in vivo*, mice were intravenously injected with ADSCs-derived exosomes before being subjected to MIRI. *In-situ* apoptosis of myocardial tissue was estimated by Tunel assay. Figure 3A showed that the count of apoptotic cardiomyocytes in the Exo group was significantly less than that in the IR group. In particular, the Int-Exo group exhibited the lowerest percentage of apoptosis (NC-Exo vs IR group; $p = 0.0003$; Int-Exo vs NC-Exo group; $p = 0.0141$).

3.6. ADSCs-derived exosomes with anoxia preconditioning reduced myocardial infarct size

Infarct size(IS) and AAR of the myocardium after MIRI in WT C57BL/6 mice pre-treated with ADSCs-derived exosomes was evaluated. Figure 3B showed that the AAR/LV between the Exo groups, IR group, and sham group mice were similar, which indicated that the models were successful and comparable. Furthermore, NC-Exo and Int-Exo groups exhibited significantly reduced infarct size compared to the IR group. Among them, the Int-Exo group had the most minimal infarct size (NC-Exo vs IR group; $p = 0.0007$; Int-Exo vs NC-Exo group; $p = 0.0028$).

3.7. Exosomes derived from ADSCs with anoxia preconditioning alleviated pyroptosis in myocardium

To confirm whether ADSCs-derived exosomes with anoxia preconditioning (Int-Exo) markedly influence pyroptosis in MIRI *in vivo*, pyroptosis pathway was detected in myocardium. As shown in Fig. 3(C-D), Compared with IR group, NC-Exo decreased the expression of TXNIP and cleaved-caspase1. Furthermore, compared with NC-Exo, Int-Exo alleviated expression of TXNIP, NLRP3 and cleaved-caspase1(TXNIP, cleaved-caspase1; NC-Exo vs IR group, $p = 0.009$, $p = 0.0078$, respectively; TXNIP, NLRP3, cleaved-caspase1, Int-Exo vs NC-Exo group, $p = 0.0042$, $p = 0.0341$, $p = 0.0287$ respectively)

3.8. Exosomes derived from ADSCs with anoxia preconditioning ameliorated apoptosis in myocardium

Influence of Int-Exo and NC-Exo on myocardium apoptosis was evaluated. As shown in Fig. 3(E-F), Int-Exo and NC-Exo decreased the protein expression of cleaved-caspase-3 and upregulated the protein expression of GATA4, Bcl-2/Bax in myocardium (NC-Exo vs IR group; GATA4, Bcl-2/Bax, cleaved-caspase-3, $p = 0.0026$, $p = 0.0001$, $p = 0.0011$, respectively; Int-Exo vs NC-Exo group; GATA4, Bcl-2/Bax, cleaved-caspase-3, $p = 0.0242$, $p = 0.027$, $p = 0.0006$, respectively) treated with anoxia-reoxygenation.

3.9. ADSCs-derived exosomes with anoxia preconditioning improved cardiac function after MIRI

Echocardiography revealed that the ejection fraction (EF) and the left ventricular fractional shortening (LVFS) in I/R mice treated with exosomes were significantly higher than those of I/R mice after 3 and 7 days of reperfusion Fig. 3(G-H), especially in the Int-Exo group (EF of 3rd day after reperfusion, NC-Exo vs IR group, p = 0.020, Int-Exo vs NC-Exo group, p = 0.036; FS of 3rd day after reperfusion, NC-Exo vs IR group, p = 0.033, Int-Exo vs NC-Exo group, p = 0.015; EF of 7th day after reperfusion, NC-Exo vs IR group, p = 0.022, Int-Exo vs NC-Exo group, p = 0.017; FS of 7th day after reperfusion, NC-Exo vs IR group, p = 0.058, Int-Exo vs NC-Exo group, p = 0.014).

3.10. Pyroptosis-related miRNAs were identified as a possible target of TXNIP

To explore the underlying mechanism leading to the higher inhibiting effect of Int-Exo on pyroptosis (when compared to NC-Exo), microRNA sequencing was performed to explore the differential expression of miRNAs in the two types of exosomes. A total of 41 miRNAs were upregulated in Int-Exo compared to NC-Exo, including 10 that were predicted by target-scan, miR, and ENCORI to associate with TXNIP. The differential expression of these miRNAs was confirmed by Realtime-PCR, which is shown in Fig. 4A-B.

3.11 TXNIP is one of the target genes of miR-224-5p

Among the 10 upregulated miRNAs predicted to associate with TXNIP, miR-224-5p was selected for further study because its upregulation was the most significant. The results of Dual Luciferase Reporter assay to detect whether TXNIP was the target gene of miR-224-5p (Fig. 4C-D), the fluorescence intensity in the miR-224-5p + TXNIP WT-3’ UTR group was significantly reduced when compared to that of other groups (p = 0.009). These results indicated that miR-224-5p regulated translation of TXNIP by targeting to 3’ UTR region of TXNIP.

3.12 miR-224-5p ameliorated apoptosis of cardiomyocytes with anoxia-reoxygenation by targeting TXNIP

A rescue study was performed to further validate whether miR-224-5p can ameliorate apoptosis in MIRI, partly by targeting the TXNIP-pyroptosis-GATA4 pathway. The results showed that miR-224-5p inhibitor decreased the expression of miR-224-5p, while increasing TXNIP expression (compared with the IR group,p = 0.022) in cardiomyocytes(Fig. 4E-F). The results of AnnexinV-PI(Fig. 4G-H) indicated that the apoptotic ratio of cardiomyocytes that underwent anoxia-reoxygenation was higher than that of the control group (p□0.0001) (Fig. 4G(a)) and 4G(b)). As the expression of miR-224-5p was suppressed, the apoptotic ratio of cardiomyocytes was further increased (compared to the IR group, p = 0.0115) (Fig. 4G(e)). Moreover, inhibition of TXNIP in cardiomyocytes that underwent anoxia-reoxygenation significantly reduced the apoptosis ratio (compared with IR group, p = 0.0025) (Fig. 4G(d)). However, if miR-224-5p is inhibited, when the expression of TXNIP is suppressed, the pro-apoptotic effect due to miR-224-5p deficiency could be reversed (compared to the IR + MiR224 Inhibitor group, p < 0.0001) (Fig. 4G(f)). These results demonstrated that miR-224-5p reduces the apoptosis of cardiomyocytes that underwent anoxia-reoxygenation, partly by targeting TXNIP.

4. Discussion

Exosomes are a efficient nanoscale-vehicles which have good characteristics such as excellent biocompatibility, low immunogenicity, and can cross through the blood-brain barrier. Given that exosomes, may “target to” specific tissue and cells, targeted delivery of small-molecule and nucleic acid drug through exosomes should result in more effective treatment and fewer nonspecific delivery. Thus, exosomes also have the potential to deliver cardioprotective non-coding RNA, cytokines and small-molecule protein for the treatment of ischemic heart disease[26]. Although great advancements have been made, clinical transformation of exosomes still exsited some problems to overcome: (1) the technology of exosome isolation is not impeccable enough to meet clinical needs, (2) a synthetic vesicle and related technologies to edit exosomal content is provoking widespread concern over its biosecurity, (3) the long-time use safety of exosomes in clinical trials remains unclear[27]. Thus, our aim is to improve the biological efficacy of exosomes by using a secure anoxia-preconditioning method, thereby improving the cardioprotective effect of exosomes derived from mesenchymal stem cells, and to further elucidate the underlying mechanisms.

Remote ischemic preconditioning (RIPC) is defined as repeated stimulation of the nonadjacent tissue, organ with transitory, noninvasive ischemia, which may reduce organ MIRI[28]. Paracrine action was partly thought to underlie the mechanism of RIPC, in which exosomes plays a core role[29], which enlightened us to treat ADSCs with intermittent anoxia. Our findings revealed that exosomes derived from ADSCs that underwent anoxia preconditioning can serve as promising carriers for suppressing the activation of the cardiac pyroptosis pathway, the latter of which is a core element in inducing myocardial apoptosis. Importantly, in this study, RNA sequencing identified that there were approximately 40 miRNAs enriched in ADSCs-derived exosomes with anoxia preconditioning. According to bioinformatic analysis, 10 of these miRNAs critically mediate the pyroptosis pathway by targeting TXNIP and stabilizing the biological function of GATA4 to suppress the apoptosis of cardiomyocytes during MIRI. Thus, it is reasonable to assume that anoxia preconditioning on ADSCs could promote cells to load more miRNAs targeting TXNIP. Furthermore, the mechanism revealed in our study may partly explain the cardioprotective effect that Int-Exo exerts to reduce apoptosis of cardiomyocytes.

GATA4, as a transcription factor, with a characteristic protein structure of the zinc finger, has been proved as a vital cardioprotective factor and an indispensable mediator of adaptability of the myocardium to external pressure. When the expression of GATA4 is suppressed, toleration and survivability of cardiomyocytes against external pressure was affected, such as cardiotoxic drug and ischemic cardiomyopathy [30]. Furthermore, upregulation of GATA-4 would invert the trend of cardiomyocytes apoptosis[31]. Consequently, GATA-4 has emerged as an a potential target spot of therapeutic intervention to ischemic cardiomyopathy[32]. As transcription factor, GATA4 can activate the transcription of Bcl-2 through directly binding to Bcl-2 promoter region and up-regulate transcriptional level of Bcl-2, which inhibit cell apoptosis through 3 aspects: (1) Bcl-2 Inhibits leakage of glutathione to against oxidation state of thiol in mitochondria to stable mitochondrial membrane potential (MMP). (2) Bcl-2 regulates function of mitochondrial permeability transition pore to inhibit the release of cytochrome c(cyt-

c) and apoptosis inducing factor(AIF). (3) Bcl-2 positions apoptosis protease activating factor-1(APAF-1) to mitochondrial membrane in order to inhibit activation of caspsase-3 by blocking the conbination of APAF-1 and cyt-c[33–35]. The results of precious studys indicated that regulating GATA-4 could ameliorate cardiomyocyte apoptosis in a early stage in a early stage when MMP appears collapse. Our data demonstrated that a relatively high-expression of GATA4 and Bcl-2 protein reduced the levels of apoptosis in cardiomyocytes and myocardium undergoing MIRI, after pretreatment with Int-Exo, which was partly induced by suppressing pyroptosis pathway and activation of caspase-1.

Recently, caspase-1 was famous for its proinflammatory function in pyroptosis pathway, videlicet, the primary molecules of execution of the pyroptosis process, during which caspase-1 cleaves and promote IL-1β, IL-18, and gasderminD (GSDMD)[36] to be activated state. Sepsis related activation of pyroptosis pathway was confirmed to have relevance to several cardiac diseases such as acute myocardial infarction, heart failure, and myocardial contractile dysfunction[37, 38]. Moreover, actived caspase-1 is a upstream regulatory molecular of GATA4 to directly induce its inactivation. It is reported that P4 position containing hydrophobic amino acid is the ideal binding site of cleaved caspase-1. It's worth noting that GATA4 protein has such characteristics in two functional sites binded and cleaved by caspase-1, that is, $YMAD^{168}$ within the major transcription activation domain and $WRRD^{230}$ within the first zinc finger were the target sites of caspase-1. Whichever the site was cleaved by caspase-1, transcriptional activity of GATA4 is bound to be affected[39]. Our findings showed that specific miRNAs transferred from Int-Exo to cardiomyocytes bound to the 3’UTR sequence of TXNIP, suppressed the pyroptosis-caspase1 pathway, thus protecting GATA4 from cleavage and alleviating apoptosis.

In most studies, various types of programmed cell death are considered independent, discrete, and unrelated. Apoptosis and pyroptosis are different in morphology, function, and mechanism[40]. On a cellular level, while membrane shrinking and the formation of vesicular bodies (apoptotic bodies) is the outcome of apoptosis. As for pyroptosis, it is a inflammasome-induced programmed cell death in form of loss of membrane permeability, membranolysis and release of inflammatory cytokines, triggered by GSDMD[41, 42]. GSDMD was defined as a functional executive molecule to cause cell death at the end of pyroptosis. Actived caspase-1 cleaves GSDMD between its N-terminal and C-terminal domains. Then the former was capable of bioactivities that actived GSDMD cause pores on cytomembrane to induce cell death[43]. Currently, it is general deemed that caspase-1 is an inflammation-related protein. A probably reason is that the majority of researches involved in inflammasomes applying inflammatory cell or myeloid cells as cell model that abundantly express GSDMD[44]. However, earlier studies indicated that actived caspase-1 could cause cell apoptosis in the deficiency of GSDMD through Bid induced cell apoptosis and other pathway [45, 46]. In fact, caspase-1 was the vital role of both GSDMD-deficient and GSDMD-abundant programmed cell death pathways, in consideration of activation of pyroptosis/caspase1 pathway could induce apoptosis rather than pyroptosis in cell types that do not or only weakly express GSDMD[47, 48]. We displayed a signal path diagram to graphically explain the pyroptosis/caspase1 induced apoptosis mediated by Int-Exo(Graphical Abstract). In our studies, as a type of non-myeloid cell, cardiomyocytes showed a relatively low expression of total GSDMD in protein degree.

Although with the activation of pyroptosis/caspase-1 pathway, the cleavage of GSDMD was also inapparent(Fig. 4), which were consistent with Tsuchiya K's results[45]. That is the deficiency of GSDMD blocks the last stage of pyroptosis-related membranolysis, thus the main manifestation of MIRI in cardiomyoctes still was apooptosis even with the activation of pyroptosis pathway. The pyroptosis/caspase-1-induced apoptosis occurs in cardiomyocytes through cleaving GATA4. Accordingly, the level of cleaved-caspase-1 in caspase-1-induced apoptosis under MIRI conditions may be inversely proportional to the expression of GATA4. Moreover, once miRNAs in Int-Exo bind and inhibit the expression of TXNIP, namely reducing the activation of the inflammasome and cleavage of caspase-1, the trend of inactivated GATA4 is reversed. The results reveal that pyroptosis-GATA4-apoptosis axis may exist and partly play a key role in ROS-induced MIRI.

Limitations still existed in our study: (1) Our results suggested exosomes derived from anoxia preconditioned ADSCs can perform a more obvious effect against MIRI, it is important to note that miRNA differences were not just limited in miRNAs targeting TXNIP, which maybe the main difference in int-Exo, such as protein, cytokines, other non-coding RNA may do anti-MIRI a favor. Thus we cannot exclude miRNAs' cardioprotection function through targeting other genes. (2) Due to the functional limitation of currently available antibody which could not specifically binding to NLRP3 and ASC protein assembled into inflammasome. Thus western blot results in this research of NLRP3 and ASC just reflected whole protein degree in cells, which may explain non-significant expression difference in NLRP3 and ASC in IR and Exo groups. Further investigations are expected to elucidate the role of exosomes in protecting cardiomyocytes from MIRI.

In conclusion, our study indicated that ADSCs-derived exosomes that undergo intermittent anoxia preconditioning exerted a more significant cardioprotective effect against MIRI, because these exosomes were loaded with higher levels of miRNAs targeting TXNIP. In addition, as non-myeloid cells, activation of the pyroptosis pathway in cardiomyocytes would induce cell apoptosis in a GSDMD-deficient form rather than pyroptosis caused by the GSDMD protein. Thus, Int-Exo worked as a more effective anti-apoptotic factor by inhibiting the activation of the inflammasome to increase expression of GATA4. These findings provide new insights into the pathogenesis of MIRI and methods for intervention at early stages of MIRI.

Ethics approval and consent to participate

All animal experiment procedures after appraisals, feasibility studies were approved by the Shanghai Ninth People's Hospital institutional ethics committee (SH9H-2017-A39-1). All experimental contents acted in accordance with the guidelines of the Directive 2010/63/EU of European Parliament.

Consent for publication

Not applicable.

Declarations

Ethics approval and consent to participate

All animal experiment procedures after appraisals, feasibility studies were approved by the Shanghai Ninth People's Hospital institutional ethics committee (SH9H-2017-A39-1). All experimental contents acted in accordance with the guidelines of the Directive 2010/63/EU of European Parliament.

Consent for publication

Not applicable.

Authors' contributions

Changqian Wang and Chengyu Mao conceived and designed the study. Chengyu Mao, Dongjiu Li,En Zhou,Erhe Gao,Tiantian Zhang performed the experiments.Lin Gao and Yue Wang wrote the paper. Yue Wang,Kan Chen reviewed and edited the manuscript. All authors read and approved the manuscript..

Competing interests

The authors declare no competing interests.

Availability of data and material

The data that support the findings of this study are available from the corresponding author upon reasonable request.

Acknowledgements and funding

This work was supported by grants from National Natural Science Foundation of China [grant number 81870264], Clinical research project of the ninth people's hospital affiliated to the Medical School of Shanghai Jiaotong University [grant number JYLJ017], Shanghai Committee of Science and Technology, China [grant number 18411950500], and a three-year action plan to promote clinical skills and innovation in municipal hospitals [grant number 16CR20348].

References

1. Hausenloy DJ, Yellon DM. Ischaemic conditioning and reperfusion injury. Nat Rev Cardiol. 2016;13:193–209.
2. Pfeffer MA, Braunwald E. Ventricular remodeling after myocardial infarction. Experimental observations and clinical implications. Circulation. 1990;81:1161–72.
3. Ravassa S, Trippel T, Bach D, Bachran D, Gonzalez A, Lopez B, Wachter R, Hasenfuss G, Delles C, Dominiczak AF, Pieske B, Diez J, Edelmann F. Biomarker-based phenotyping of myocardial fibrosis identifies patients with heart failure with preserved ejection fraction resistant to the beneficial effects of spironolactone: results from the Aldo-DHF trial. Eur J Heart Fail. 2018;20:1290–9.

4. Chen YR, Zweier JL. Cardiac mitochondria and reactive oxygen species generation. Circulation research. 2014;114:524–37.
5. Huang C, Liu Y, Beenken A, Jiang L, Gao X, Huang Z, Hsu A, Gross GJ, Wang YG, Mohammadi M, Schultz JEJ. A novel fibroblast growth factor-1 ligand with reduced heparin binding protects the heart against ischemia-reperfusion injury in the presence of heparin co-administration. Cardiovascular research. 2017;113:1585–602.
6. Zhang B, Novitskaya T, Wheeler DG, Xu Z, Chepurko E, Huttinger R, He H, Varadharaj S, Zweier JL, Song Y, Xu M, Harrell FE Jr, Su YR, Absi T, Kohr MJ, Ziolo MT, Roden DM, Shaffer CM, Galindo CL, Wells QS, Gumina RJ, Kcnj11 Ablation Is Associated With Increased Nitro-Oxidative Stress During Ischemia-Reperfusion Injury: Implications for Human Ischemic Cardiomyopathy, Circulation. Heart failure, 10 (2017).
7. Li H, Xia Z, Chen Y, Qi D, Zheng H, Mechanism and Therapies of Oxidative Stress-Mediated Cell Death in Ischemia Reperfusion Injury, Oxidative medicine and cellular longevity, 2018 (2018) 2910643.
8. Aries A, Whitcomb J, Shao W, Komati H, Saleh M, Nemer M. Caspase-1 cleavage of transcription factor GATA4 and regulation of cardiac cell fate. Cell death disease. 2014;5:e1566.
9. Merkle S, Frantz S, Schon MP, Bauersachs J, Buitrago M, Frost RJ, Schmitteckert EM, Lohse MJ, Engelhardt S. A role for caspase-1 in heart failure. Circulation research. 2007;100:645–53.
10. Aries A, Paradis P, Lefebvre C, Schwartz RJ, Nemer M. Essential role of GATA-4 in cell survival and drug-induced cardiotoxicity. Proc Natl Acad Sci USA. 2004;101:6975–80.
11. Cui Y, Xu H-F, Liu M-Y, Xu Y-J, He J-C, Zhou Y, Cang S-D. Mechanism of exosomal microRNA-224 in development of hepatocellular carcinoma and its diagnostic and prognostic value. World J Gastroenterol. 2019;25:1890–8.
12. Hazan-Halevy I, Rosenblum D, Weinstein S, Bairey O, Raanani P, Peer D. Cell-specific uptake of mantle cell lymphoma-derived exosomes by malignant and non-malignant B-lymphocytes. Cancer letters. 2015;364:59–69.
13. Zhang Y, Liu Y, Liu H, Tang WH. Exosomes: biogenesis, biologic function and clinical potential. Cell bioscience. 2019;9:19.
14. Yellon DM, Davidson SM. Exosomes: nanoparticles involved in cardioprotection? Circulation research. 2014;114:325–32.
15. Yang PC. Induced Pluripotent Stem Cell (iPSC)-Derived Exosomes for Precision Medicine in Heart Failure. Circulation research. 2018;122:661–3.
16. Bang C, Batkai S, Dangwal S, Gupta SK, Foinquinos A, Holzmann A, Just A, Remke J, Zimmer K, Zeug A, Ponimaskin E, Schmiedl A, Yin X, Mayr M, Halder R, Fischer A, Engelhardt S, Wei Y, Schober A, Fiedler J, Thum T. Cardiac fibroblast-derived microRNA passenger strand-enriched exosomes mediate cardiomyocyte hypertrophy. J Clin Investig. 2014;124:2136–46.
17. Yang J, Yu X, Xue F, Li Y, Liu W, Zhang S. Exosomes derived from cardiomyocytes promote cardiac fibrosis via myocyte-fibroblast cross-talk. American journal of translational research. 2018;10:4350–66.

18. Broughton KM, Sussman MA. Enhancement Strategies for Cardiac Regenerative Cell Therapy: Focus on Adult Stem Cells. Circulation research. 2018;123:177–87.
19. Pei M. Environmental preconditioning rejuvenates adult stem cells' proliferation and chondrogenic potential. Biomaterials. 2017;117:10–23.
20. Zhang X, Zhang JH, Chen XY, Hu QH, Wang MX, Jin R, Zhang QY, Wang W, Wang R, Kang LL, Li JS, Li M, Pan Y, Huang JJ, Kong LD. Reactive oxygen species-induced TXNIP drives fructose-mediated hepatic inflammation and lipid accumulation through NLRP3 inflammasome activation. Antioxid Redox Signal. 2015;22:848–70.
21. Katsu-Jiménez Y, Vázquez-Calvo C, Maffezzini C, Halldin M, Peng X, Freyer C, Wredenberg A, Giménez-Cassina A, Wedell A, Arnér ESJ, Absence of TXNIP in Humans Leads to Lactic Acidosis and Low Serum Methionine Linked to Deficient Respiration on Pyruvate, Diabetes, 68 (2019) 709–723.
22. Gao E, Lei YH, Shang X, Huang ZM, Zuo L, Boucher M, Fan Q, Chuprun JK, Ma XL, Koch WJ. A novel and efficient model of coronary artery ligation and myocardial infarction in the mouse. Circulation research. 2010;107:1445–53.
23. Salehi PM, Foroutan T, Javeri A, Taha MF. Extract of mouse embryonic stem cells induces the expression of pluripotency genes in human adipose tissue-derived stem cells. Iranian journal of basic medical sciences. 2017;20:1200–6.
24. Ehler E, Moore-Morris T, Lange S, Isolation and culture of neonatal mouse cardiomyocytes, Journal of visualized experiments: JoVE, (2013).
25. Lee K, Shao H, Weissleder R, Lee H. Acoustic purification of extracellular microvesicles. ACS Nano. 2015;9:2321–7.
26. Shah K. Stem cell-based therapies for tumors in the brain: are we there yet? Neurooncology. 2016;18:1066–78.
27. Zhang L, Yu D. Exosomes in cancer development, metastasis, and immunity, Biochimica et biophysica acta. Reviews on cancer. 2019;1871:455–68.
28. Zwaag J, Beunders R, Warlé MC, Kellum JA, Riksen NP, Pickkers P, Kox M. Remote ischaemic preconditioning does not modulate the systemic inflammatory response or renal tubular stress biomarkers after endotoxaemia in healthy human volunteers: a single-centre, mechanistic, randomised controlled trial. Br J Anaesth. 2019;123:177–85.
29. Liu W, Rong Y, Wang J, Zhou Z, Ge X, Ji C, Jiang D, Gong F, Li L, Chen J, Zhao S, Kong F, Gu C, Fan J, Cai W. Exosome-shuttled miR-216a-5p from hypoxic preconditioned mesenchymal stem cells repair traumatic spinal cord injury by shifting microglial M1/M2 polarization. J Neuroinflamm. 2020;17:47.
30. Oka T, Maillet M, Watt AJ, Schwartz RJ, Aronow BJ, Duncan SA, Molkentin JD. Cardiac-specific deletion of Gata4 reveals its requirement for hypertrophy, compensation, and myocyte viability. Circulation research. 2006;98:837–45.
31. Suzuki YJ, Evans T. Regulation of cardiac myocyte apoptosis by the GATA-4 transcription factor, Life sciences, 74 (2004) 1829–1838.

32. Li HX, Zhou YF, Zhao X, Jiang B, Yang XJ. GATA-4 protects against hypoxia-induced cardiomyocyte injury: effects on mitochondrial membrane potential. Can J Physiol Pharmacol. 2014;92:669–78.
33. Kobayashi S, Lackey T, Huang Y, Bisping E, Pu WT, Boxer LM, Liang Q. Transcription factor gata4 regulates cardiac BCL2 gene expression in vitro and in vivo, FASEB journal: official publication of the Federation of American Societies for Experimental Biology, 20 (2006) 800–802.
34. Kyronlahti A, Ramo M, Tamminen M, Unkila-Kallio L, Butzow R, Leminen A, Nemer M, Rahman N, Huhtaniemi I, Heikinheimo M, Anttonen M. GATA-4 regulates Bcl-2 expression in ovarian granulosa cell tumors. Endocrinology. 2008;149:5635–42.
35. Zhang N, Ye F, Zhu W, Hu D, Xiao C, Nan J, Su S, Wang Y, Liu M, Gao K, Hu X, Chen J, Yu H, Xie X, Wang J. Cardiac ankyrin repeat protein attenuates cardiomyocyte apoptosis by upregulation of Bcl-2 expression, Biochimica et biophysica acta, 1863 (2016) 3040–3049.
36. Denes A, Lopez-Castejon G, Brough D. Caspase-1: is IL-1 just the tip of the ICEberg? Cell death disease. 2012;3:e338.
37. Mezzaroma E, Toldo S, Farkas D, Seropian IM, Van Tassell BW, Salloum FN, Kannan HR, Menna AC, Voelkel NF, Abbate A. The inflammasome promotes adverse cardiac remodeling following acute myocardial infarction in the mouse. Proc Natl Acad Sci USA. 2011;108:19725–30.
38. Bracey NA, Beck PL, Muruve DA, Hirota SA, Guo J, Jabagi H, Wright JR Jr, Macdonald JA, Lees-Miller JP, Roach D, Semeniuk LM, Duff HJ. The Nlrp3 inflammasome promotes myocardial dysfunction in structural cardiomyopathy through interleukin-1beta. Exp Physiol. 2013;98:462–72.
39. Aries A, Whitcomb J, Shao W, Komati H, Saleh M, Nemer M. Caspase-1 cleavage of transcription factor GATA4 and regulation of cardiac cell fate. Cell death disease. 2014;5:e1566.
40. Sun L, Ma W, Gao W, Xing Y, Chen L, Xia Z, Zhang Z, Dai Z. Propofol directly induces caspase-1-dependent macrophage pyroptosis through the NLRP3-ASC inflammasome. Cell death disease. 2019;10:542.
41. Malik A, Kanneganti TD. Inflammasome activation and assembly at a glance. Journal of cell science. 2017;130:3955–63.
42. 42.
43. Ding J, Wang K, Liu W, She Y, Sun Q, Shi J, Sun H, Wang DC, Shao F. Pore-forming activity and structural autoinhibition of the gasdermin family. Nature. 2016;535:111–6.
44. He W-t, Wan H, Hu L, Chen P, Wang X, Huang Z, Yang Z-H, Zhong C-Q, Han J. Gasdermin D is an executor of pyroptosis and required for interleukin-1β secretion. Cell Res. 2015;25:1285–98.
45. Tsuchiya K, Nakajima S, Hosojima S, Thi Nguyen D, Hattori T, Manh Le T, Hori O, Mahib MR, Yamaguchi Y, Miura M, Kinoshita T, Kushiyama H, Sakurai M, Shiroishi T, Suda T, Caspase-1 initiates apoptosis in the absence of gasdermin D, Nature communications, 10 (2019) 2091.
46. Miura M, Zhu H, Rotello R, Hartwieg EA, Yuan J, Induction of apoptosis in fibroblasts by IL-1 beta-converting enzyme, a mammalian homolog of the C. elegans cell death gene ced-3, Cell, 75 (1993) 653–660.

47. Kayagaki N, Stowe IB, Lee BL, O'Rourke K, Anderson K, Warming S, Cuellar T, Haley B, Roose-Girma M, Phung QT, Liu PS, Lill JR, Li H, Wu J, Kummerfeld S, Zhang J, Lee WP, Snipas SJ, Salvesen GS, Morris LX, Fitzgerald L, Zhang Y, Bertram EM, Goodnow CC, Dixit VM. Caspase-11 cleaves gasdermin D for non-canonical inflammasome signalling. Nature. 2015;526:666–71.
48. He WT, Wan H, Hu L, Chen P, Wang X, Huang Z, Yang ZH, Zhong CQ, Han J. Gasdermin D is an executor of pyroptosis and required for interleukin-1beta secretion. Cell Res. 2015;25:1285–98.

Figures

Fig1

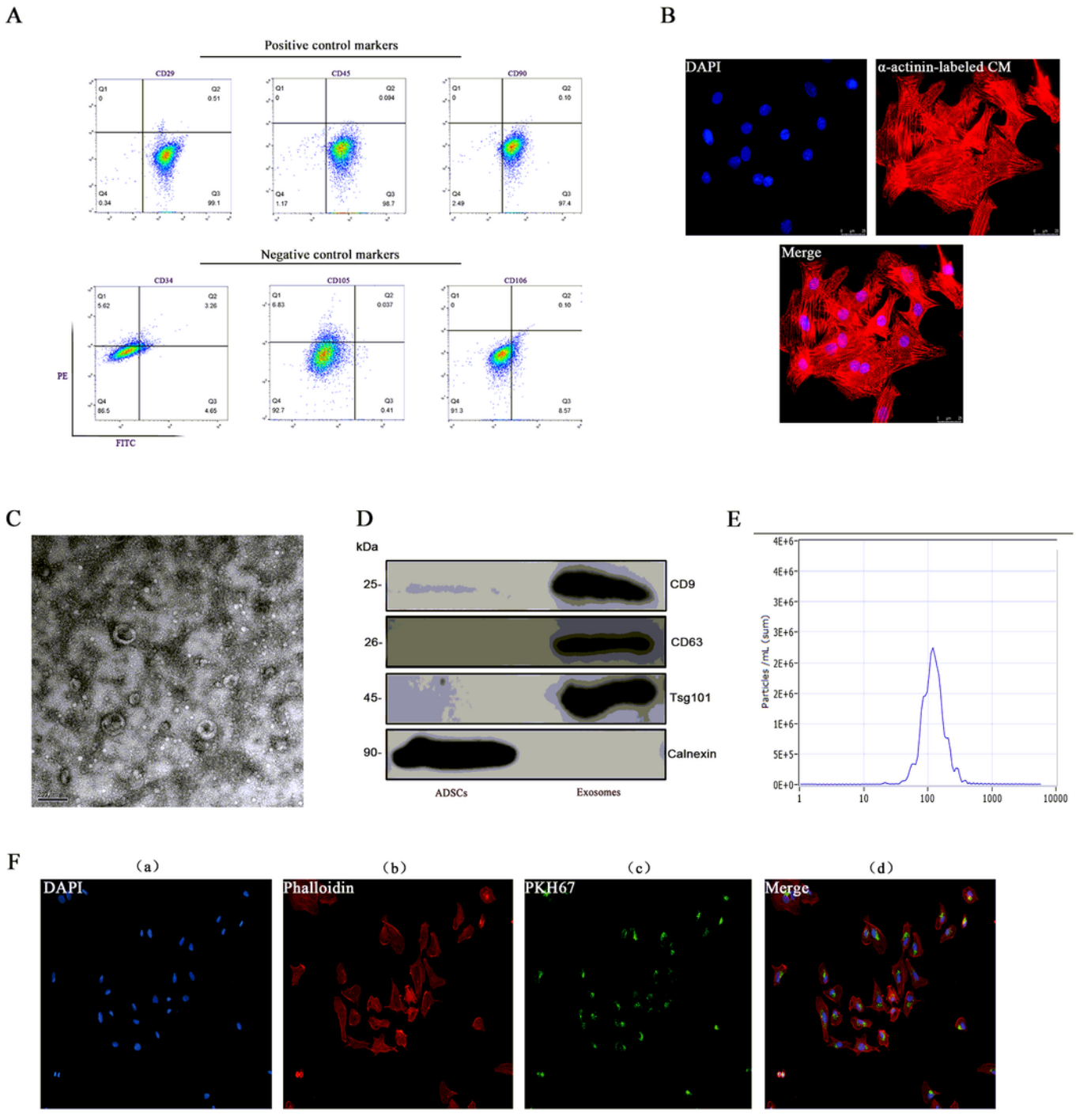

Figure 1

Identification of ADSCs and ADSCs-derived exosomes A)CD29, CD45, and CD90 were used as cell surface markers; CD34, CD105, and CD106 were used as negative controls. B) The purity of neonatal mice cardiomyocytes was estimated to be higher than 95% based on the results of the α-actinin staining. C) TEM characterization of exosomes. D) Western blot examination of exosome biomarkers in ADSCs-derived exosomes and ADSCs calnexin were used as negative control. E) Size distribution by intensity

was detected through nanosight. F) Exosome tracer assay was used to identify exosomes that were absorbed by cells.

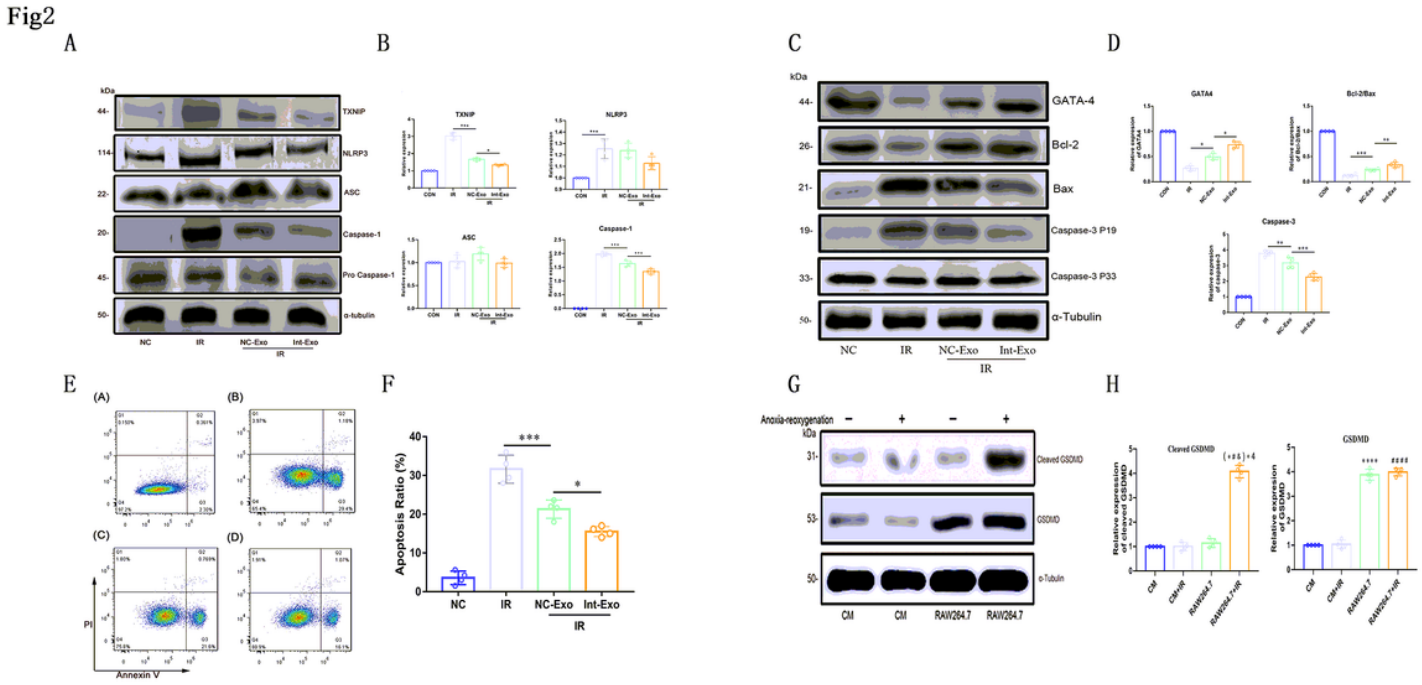

Figure 2

Cardioprotective effects of ADSCs-derived exosomes in vitro studies A-B) Relative expression of cleaved GSDMD and total GSDMD of cardiomyocytes and RAW264.7 treated or without being treated with anoxia/ reoxygenation (Compared with the CM group,*P < 0.05, **P < 0.01, *** P < 0.001, **** P < 0.0001, n = 4); (Compared with the CM+IR group #P < 0.05, ##P < 0.01,###P < 0.001, #### P < 0.0001, n = 4,); (Compared with the RAW264.7 group, &P < 0.05, &&P < 0.01, &&& P < 0.001, &&&&P < 0.0001, n = 4). C-D) Based on Western blot results, Int-Exo and NC-Exo decreased the expression of TXNIP, and cleaved-caspase-1 protein in cardiomyocytes treated with anoxia-reoxygenation. NC-Exo group was compared with the IR group, Int-Exo group was compared with the NC-Exo group (*P < 0.05, **P < 0.01, *** P < 0.001, **** P < 0.0001, n = 4). E-F) According to Western blot results, Int-Exo and NC-Exo decreased the expression of BAX and cleaved-caspase-3 protein and upregulated the expression of GATA4 and Bcl-2 protein in cardiomyocytes treated with anoxia-reoxygenation. NC-Exo group was compared with the IR group, Int-Exo group was compared with the NC-Exo group (*P < 0.05, **P < 0.01, *** P < 0.001, **** P < 0.0001, n = 4). G-H) Descending trend of apoptotic cell ratio was detected in Int-Exo and NC-Exo groups by Annexin V-PI assay. NC-Exo group was compared with the IR group, Int-Exo group was compared with the NC-Exo group (*P < 0.05, **P < 0.01, *** P < 0.001, **** P < 0.0001, n = 4).

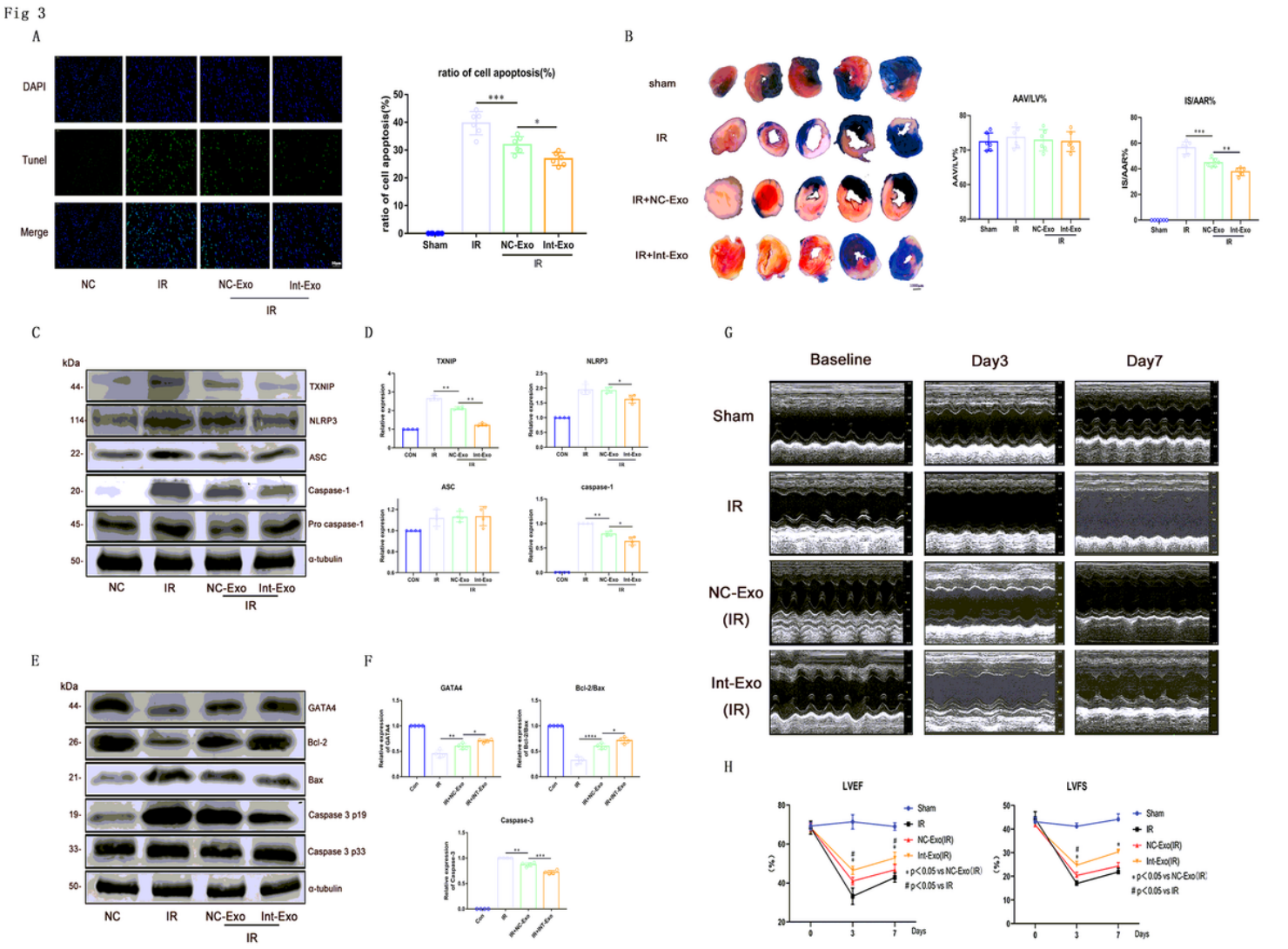

Figure 3

Cardioprotective effects of ADSCs-derived exosomes in vivo mice model of MIRI A) Int-Exo and NC-Exo alleviated cardiomyocyte apoptosis of infarcted tissue after MIRI in situ apoptosis was determined using a TUNEL assay. NC-Exo group was compared with the IR group, Int-Exo group was compared with the NC-Exo group (zoom below: 400× magnification, *P < 0.05, **P < 0.01, *** P < 0.001, **** P < 0.0001, n = 6). B) Int-Exo and NC-Exo decreased infarction size of wild-type (WT) C57BL/6 mice subjected to I/R; AAR and infarct size were subsequently measured using Evans Blue/TTC staining. NC-Exo group was compared with the IR group, Int-Exo group was compared with the NC-Exo group (10× magnification, IR: ischemia reperfusion; TTC: triphenyltetrazolium chloride; AAR: area at risk; IS: infarction size, *P < 0.05, **P < 0.01, *** P < 0.001, **** P < 0.0001, n = 6). C-D) Int-Exo and NC-Exo decreased expression of TXNIP, cleaved-caspase-1 protein and Int-Exo decreased expression of NLRP3 compared with NC-Exo group in infarcted tissue of mice model of MIRI, as detected by Western Blot. NC-Exo group was compared with the IR group, Int-Exo group was compared with the NC-Exo group□*P < 0.05, **P < 0.01, *** P < 0.001, **** P < 0.0001, n = 4). E-F□Int-Exo and NC-Exo decreased the expression of BAX and cleaved-caspase-3

protein, and upregulated the expression of GATA4 and Bcl-2 protein in infarcted tissue of a mice model of MIRI.. NC-Exo group was compared with the IR group, Int-Exo group was compared with the NC-Exo group （*P < 0.05, **P < 0.01, *** P < 0.001, **** P < 0.0001, n = 4). G-H：Int-Exo and NC-Exo improved cardiac function. Echocardiography was used to examine the heart function of sham, IR, Int-Exo, and NC-Exo group mice after MIRI at baseline, and the third and seventh days after reperfusion; EF and FS were detected. NC-Exo group was compared with the IR group (#P < 0.05, ##P < 0.01, ### P < 0.001, #### P < 0.0001, n = 7). Int-Exo group was compared with the NC-Exo group (*P < 0.05, **P < 0.01, *** P < 0.001, **** P < 0.0001, n = 7). Statistical analysis was performed using Pearson Chi square test(n≥5) or Fisher exact test（n＜5）with subsequent multiple comparisons using Chi square with Bonferroni correction for categorical variables. One-way ANOVA with subsequent post hoc multiple comparisons using the Student-Newman-Keuls test for continuous variables.

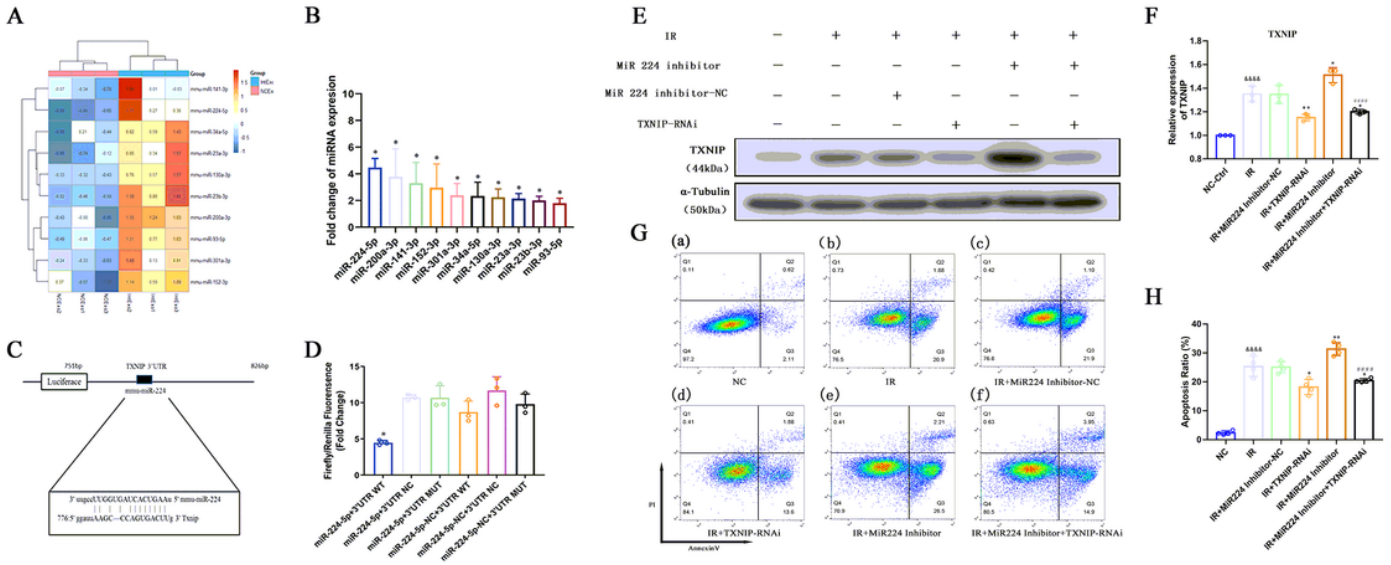

Figure 4

Mir-224-5p partially abolished activation of the TXNIP-inflammasome pathway to upregulate expression of GATA4, which alleviated apoptosis in cardiomyocyte by targeting TXNIP A：MicroRNA sequencing was performed to explore the differential expression of miRNAs in NC-Exo and Int-Exo. A total of 41 miRNAs were upregulated in Int-Exo, 10 of them were predicted by target-scan, miR, and ENCORI to associate with TXNIP. The heatmap showed 10 MiRNAs targeting TXNIP genes. B) The differential expression of miRNAs in NC-Exo and Int-Exo was detected through qRT-PCR, with U6 snRNA as an internal reference (compared with the NC-Exo group, *P < 0.05, n=3). C) 293 T cells were transfected with PGL3 luciferase reporter plasmids containing wild-type or mutated TXNIP 3'UTR and miR-224-5p mimics, using NC as controls. D) The miR-224-5p+TXNIP 3'UTR WT group was compared with other groups, *P < 0.05, n=3). E) TXNIP-RNAi downregulated the expression of TXNIP in a mice cardiomyocyte model of anoxia-reoxygenation, which was upregulated by an MiR224-5p inhibitor. F) Compared with the control group (&P < 0.05, &&P < 0.01, &&& P < 0.001, &&&&P < 0.0001, n = 3); Compared with the IR group（*P < 0.05, **P < 0.01, *** P < 0.001, **** P < 0.0001, n = 3); Compared with the IR+inhibitor group (#P < 0.05, ##P < 0.01,

P < 0.001, #### P < 0.0001, n = 3). G) The MiR224-5p inhibitor increased the apoptosis of mice cardiomyocytes after anoxia and re-oxygenation, which was decreased by TXNIP-RNAi. (a) CON group: mice cardiomyocyte; (b). IR group: mice cardiomyocyte that experienced anoxia and re-oxygenation; (c). Inhibitor-NC + IR group: mice cardiomyocytes were stimulated with the MiR224-5p inhibitor (negative control) and then experienced hypoxia and re-oxygenation; (d). TXNIP-RNAi + IR group: mice cardiomyocytes were treated with TXNIP-RNAi. Then, these mice cardiomyocytes were stimulated with anoxia and re-oxygenation; (e). Inhibitor + IR group: mice cardiomyocyte were stimulated with the MiR224-5p inhibitor and then experienced anoxia and re-oxygenation; (f). Inhibitor + TXNIP-RNAi + IR group: mice cardiomyocytes were treated with the MiR224-5p inhibitor and then transfected with TXNIP-RNAi. Then, cardiomyocytes were stimulated with anoxia and re-oxygenation. H). Compared with the control group (&P < 0.05, &&P < 0.01, &&& P < 0.001, &&&&P < 0.0001, n = 4); Compared with IR group(*P < 0.05, **P < 0.01, *** P < 0.001, **** P < 0.0001, n = 4); Compared with IR+MiR224 inhibitor (#P < 0.05, ##P < 0.01, ### P < 0.001, #### P < 0.0001, n = 4). Statistical analysis was performed using Pearson Chi square test(n≥5) or Fisher exact test□n□5□with subsequent multiple comparisons using Chi square with Bonferroni correction for categorical variables. One-way ANOVA with subsequent post hoc multiple comparisons using the Student-Newman-Keuls test for continuous variable.

Supplementary Files

This is a list of supplementary files associated with this preprint. Click to download.

- GraphicalAbstract.tif